



A Carbazole-based Fluorescent Turn-off Chemosensor for Iron (II/III) Detection in a Dimethyl Sulfoxide

Ahmet Battal¹ · Solomon Bezabeh Kassa² · Nuray Altinolcek Gultekin³ · Mustafa Tavasli³ · Yavuz Onganer²

Received: 22 December 2022 / Accepted: 23 January 2023 / Published online: 31 January 2023
© The Author(s), under exclusive licence to Springer Science+Business Media, LLC, part of Springer Nature 2023

Abstract

We designed a novel carbazole-based chemosensor from 2-(N-hexylcarbazol-3'-yl)-pyridine-5-carbaldehyde which was named probe **7b**. The main purpose of this study is to investigate whether metal ions in liquid media can be detected with probe **7b**. The details were presented in this paper. First, the molecular absorption and fluorescence properties of probe **7b** were characterized by spectrophotometers. Then, several methods were applied to check its sensing properties. The results showed that probe **7b** has a sense towards Fe³⁺ ion than other interfering metal ions. The selectivity and sensitivity of probe **7b** towards Fe³⁺ were very satisfactory to use in applications. Also, it was observed that when aqueous Fe³⁺ ion solutions were added to probe **7b** in dimethyl sulfoxide (DMSO), the fluorescence intensity of probe **7b** decreased. This situation (turn-off of emission) is due to the paramagnetic effect between probe **7b** and Fe³⁺ ions. The limit of detection (LOD) value was found as 1.38 nM for probe **7b**. This value is very small to compete with its counterparts in the literature. A real sample experiment indicated that probe **7b** can detect Fe³⁺ ions more than other ions in real media, too. As a result, it was deduced that probe **7b** is a very strong candidate to use in sensor technology.

Keywords Carbazole Fluorescent Chemosensor Fe³⁺ ion Real sample Probe

Introduction

Throughout history, iron compared to other metals is one of the most used transition metals everywhere like buildings, items, vehicles, etc. [1]. While iron makes life easier like in big residences due to its strong and tough structure, it is an essential element for human life at the same time. Thus, the iron mineral found in biological organisms is taking on various tasks. These tasks are the production of red blood cells, regulation of gene expression, oxygen metabolism, transcriptional regulation, energy production, synthesis of DNA

and RNA, electron and oxygen transport, cellular immunity in humans, etc. [1–4]. Iron minerals can be found in the form of ferric (Fe³⁺) or ferrous (Fe²⁺) in the human body [5]. This feature makes also them necessary and beneficial for human life regarding electron exchange [6]. Meanwhile, the WHO suggests that the secure level of iron is 2 mg/mL for the human body [7]. Consequently, iron levels in our bodies must be determined correctly. Excess iron causes the formation of free oxygen radicals, cancer, and Alzheimer's disease [1–4, 8]. On the other hand, its deficiency creates serious health problems such as Parkinson's, anemia, diabetes, and liver damage [1, 2, 6, 8, 9]. Hence, the accurate detection of Fe³⁺ metal ions is especially very crucial for life safety.

Nowadays, there are many methods used for iron detection. The most widespread are colorimetry, electrochemistry, mass spectroscopy, liquid chromatography and electrochemical methods [9, 10]. However, fluorescence sensors have become more advantageous to other methods recently due to their sensitivity [1, 9], easy use and equipment [11], cheap and fast [2, 12], selectivity [1, 8], reliability [4] and working in both liquid and non-liquid media [1]. Hence, highly selective fluorescent chemosensors for Fe³⁺ and/

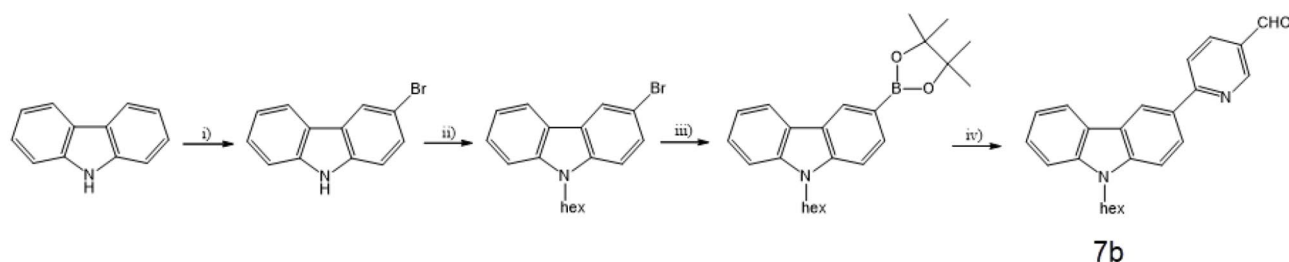
✉ Mustafa Tavasli
mtavasli@uludag.edu.tr

✉ Yavuz Onganer
yonganer@atauni.edu.tr

¹ Department of Elementary School of Education, Faculty of Education, Muş Alparslan University, 49100 Muş, Turkey

² Department of Chemistry, Faculty of Science, Atatürk University, 25240 Erzurum, Turkey

³ Department of Chemistry, Faculty of Science-Art, Uludağ University, 16059 Nilufer, Bursa, Turkey



Scheme 1 Synthesis of the compound **7b**

or Fe^{2+} are devoted to more investigation owing to these remarkable advantages [1, 2, 6, 9, 11, 13, 14].

Carbazole and its derivatives have been mostly used for the recognition of iron and other metal ions [6, 13, 15–18]. Such compounds have many advantages, for instance; electropolymerization ability [11], good conjugated system [13], strong intramolecular charge transfer, high stability and solubility, and easy modification [1, 13]. Meanwhile, these compounds have also found a wide area of applications at electroactive applications ranging from OLEDs [19], to solar cells [20], chemiluminescence [21] and sensors [2, 6, 13, 20]. Although many several published reports regarding the detection of iron(III) ion in which carbazole-based molecules were used as a probe [2, 6, 13], as far as we know, carbazole fluorescence chemosensor with pyridine group as a spacer has not been published to detect iron(III) ion.

Consequently, in this study, we decided to investigate the metal ions sensing properties of 2-(N-hexylcarbazol-3'-yl)pyridine-5-carbaldehyde (probe **7b**), the synthesis of which was previously reported by our co-workers [22]. Herein, probe **7b** was designed with carbazole, pyridine and aldehyde units where each one acts as a fluorophore, spacer and receptor units, respectively, similar to those of the literature [11].

Experimental Section

Materials and Preparation Methods

All solvents and reagents to synthesize compound **7b** had been purchased as ACS reagents, $\geq 99.9\%$ (GC) from Sigma-Aldrich, Merck and Alfa Aesar companies and used without further purifications. All metal salts such as KCl, ZnCl_2 , HgCl_2 , AlCl_3 , $\text{CrCl}_3 \cdot 6\text{H}_2\text{O}$, FeCl_3 , $\text{MnCl}_2 \cdot 4\text{H}_2\text{O}$, $\text{MgCl}_2 \cdot 6\text{H}_2\text{O}$, $\text{CaCl}_2 \cdot 2\text{H}_2\text{O}$, $\text{CoCl}_2 \cdot 6\text{H}_2\text{O}$, $\text{Pb}(\text{CH}_3\text{COO})_2 \cdot 3\text{H}_2\text{O}$, LiCl, $\text{BaCl}_2 \cdot 2\text{H}_2\text{O}$, AgNO_3 , $\text{CuCl}_2 \cdot 2\text{H}_2\text{O}$, CdCl_2 , $\text{FeSO}_4 \cdot 7\text{H}_2\text{O}$, NaCl and $\text{Ni}(\text{NO}_3)_2 \cdot 6\text{H}_2\text{O}$ were also purchased from the VWR company as anhydrous and granular with high purity. Deionized water was used throughout the preparation of stock

solutions for all metal salts. All solutions were prepared by pipettes with different volumes.

Synthesis of Compound **7b**

In the present work, we used **7b**, 2-(N-hexylcarbazol-3'-yl)pyridine-5-carbaldehyde, where 5-pyridine-carboxyaldehyde was attached to the 3-position of carbazole via the 2-position of the pyridine ring, as chemosensor compound. Full details of the synthesis to compound **7b** (Scheme 1) can be found elsewhere [22]. Therefore, we designated compound **7b** as probe **7b** for this study.

Compound **7b** was previously synthesized and fully characterized by $^1\text{H-NMR}$, $^{13}\text{C-NMR}$ and elemental analysis techniques. All analyses were compared with the previously reported data. The relative PLQY of compound **7b** calculated in dichloromethane was found to be very high (97.4%) [22]. Meanwhile, compound **7b** had also a very large Stokes shift (136 nm) between absorption and emission spectra [22]. These results encouraged us to individually investigate the sensing properties of probe **7b** towards metal ions.

Characterization and Instrumentation

The UV-Vis absorption studies of probe **7b** were performed using the Perkin Elmer Lambda 35 UV-Vis Spectrophotometer. Also, the fluorescence measurements (PL) of the samples were carried out by the Shimadzu RF-5301PC Spectrofluorophotometer. The fluorescence spectra of probe **7b** were studied by adjusting the excitation and emission slit width of 3 nm. All UV and PL spectral characterizations were carried out within a 10 mm quartz cuvette at room temperature. UV-Vis spectrum was recorded between the wavelength range of 250–600 nm. All the samples were excited at 374 nm and the PL spectra were also collected in the wavelength range of 350–700 nm.

Fluorescence Chemosensing Capability of Probe **7b**

The stock solution (1.0×10^{-3} M) of probe **7b** was prepared in DMSO solvent and the stock solution was mixed

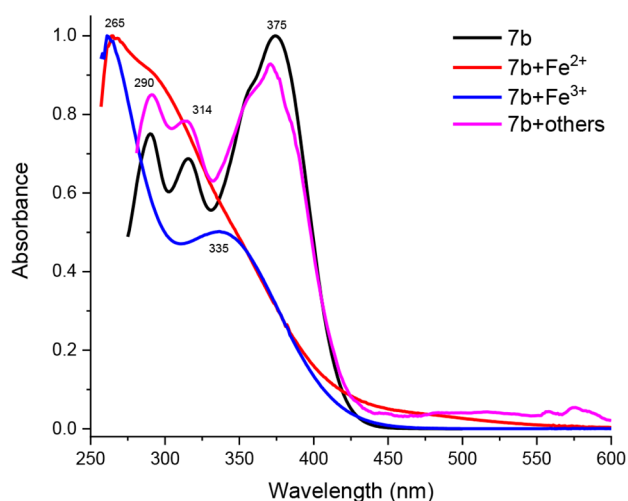


Fig. 1 UV-Vis spectra of probe **7b** in dimethyl sulfoxide at room temperature without or with various metal ions

ultrasonically for 5 min. Then, by a dilution method, a 1.0×10^{-6} M solution of probe **7b** was prepared from 1.0×10^{-5} M solution of probe **7b** which was in turn prepared from the stock solution.

For selectivity studies, 0.01 M aqueous stock solution of several metal ions (K^+ , Zn^{2+} , Hg^{2+} , Al^{3+} , Cr^{3+} , Fe^{3+} , Mn^{2+} , Mg^{2+} , Ca^{2+} , Co^{2+} , Pb^{2+} , Li^+ , Ba^{2+} , Ag^+ , Cu^{2+} , Cd^{2+} , Fe^{2+} , Na^+ and Ni^{2+}) were prepared and each time, 120 μ L of a metal ion solution was mixed with a 3 mL of probe **7b** solution in a quartz cuvette. Moreover, interference studies of probe **7b** towards Fe^{3+} in the presence of various metal ions were also carried out in the same way. The sensitivity study was performed by adding different concentrations of Fe^{3+} and Fe^{2+} ions (0–364 μ M) to a 3 mL solution of probe **7b** and incubated for 2 min at room temperature and a fixed pH value of 4.32. After these, absorption and fluorescence spectra were recorded.

Moreover, the proposed method was applied for the detection of Fe^{3+} in three different real-world water samples such as tap water, lake water and river water. The tap water and river water were collected from Muş province in Türkiye, and the lake water was also collected from Van province in Türkiye. All the water samples were centrifuged (8500 rpm, 20 min) and then filtered through 0.45 μ M membrane to remove the suspended particles. The analyses of

Fe^{3+} ions in these three different water samples were evaluated by fluorescence spectroscopy using probe **7b**.

Results and Discussions

UV-Vis Absorption Studies

The absorption properties of probe **7b** in dimethyl sulfoxide were investigated previously [22] and found that it had three specific absorption bands at 290 nm, 314 and 375 nm. These bands relate to different transition systems. The peak at 375 nm was assigned to an intramolecular charge transfer (ICT) transition. Also, in the present work, we looked at the absorption behaviour of probe **7b** in the presence of different metal ions (364 μ M).

The absorption spectra of probe **7b** in the presence of different metal ions at room temperature were depicted in Fig. 1. As shown in Fig. 1, the probe **7b** in the presence of most of the metal ions studied, except Fe^{3+} and Fe^{2+} ions, displayed similar absorption bands to the absorption band of probe **7b**. However, in the presence of Fe^{3+} and Fe^{2+} ions, the characteristic ICT band of probe **7b** showed a blue shift from 375 nm to around 335 nm. Also, a small variation occurred at high-energy bands. This result indicated that the absorption spectra of probe **7b** were not affected in the presence of most of the metal ions studied, except Fe^{3+} and Fe^{2+} .

Also, a clear probe **7b** solution turned into a light yellow solution only when the solution of Fe^{3+} and Fe^{2+} ions were added. A daylight photograph taken was depicted in Fig. 2.

Fluorescence Studies

Basic Fluorescence of Probe 7b

As it was reported previously [22], when probe **7b** in DMSO was excited at a wavelength of 375 nm, it emitted an emission at 509 nm. This emission was found to be sensitive to the polarity of solvent used, indicating the emission is from ICT band [22, 23]. This result was obtained with Duetta Fluorescence and Absorbance Spectrometer. In our

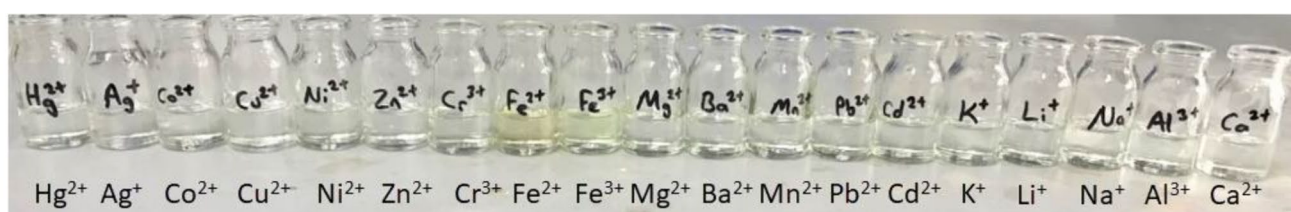


Fig. 2 Photograph of a solution of probe **7b** in the presence of various metal ions under daylight

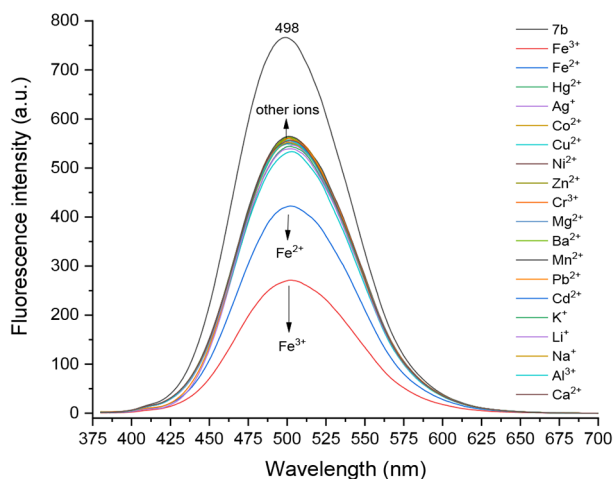


Fig. 3 Fluorescence spectra of probe **7b** in dimethyl sulfoxide at room temperature without or with various aqueous metal ions

measurements, as depicted in Fig. 3, the fluorescence spectrum of probe **7b** gave a main PL emission peak at 498 nm.

Selectivity Properties of Probe **7b** to Metal Ions

To investigate the selectivity of probe **7b** versus various metal cations, an aqueous solution of various metal ions was added to the solution of probe **7b** in DMSO. Then, the PL emission was measured at room temperature after incubating for 2 min. From various solvents probe **7b** exhibited only good response to iron ions in DMSO. Addition of water (345 μM) quenched the emission of probe **7b**, without the presence of metal ions. Thus, all experiments were carried out in DMSO.

When an aqueous solution of various metal cations such as Hg^{2+} , Ag^+ , Co^{2+} , Cu^{2+} , Ni^{2+} , Zn^{2+} , Cr^{3+} , Mg^{2+} , Ba^{2+} , Mn^{2+} , Pb^{2+} , Cd^{2+} , K^+ , Li^+ , Na^+ , Al^{3+} , Ca^{2+} was added to the solution of probe **7b**, PL emission decreased slightly due to small interaction with probe **7b** as shown in Fig. 3. However, the PL emission of probe **7b** was quenched with the addition of Fe^{3+} and Fe^{2+} . Similar observations were made by others for different probes [6, 7]. Since the paramagnetic effect for metal sensor application is very oppressive, the fluorescence

of probe **7b** was possibly quenched through electron and/or energy transfer mechanisms [7]. It can be said that an adduct may have formed because of the reaction between the probe **7b** and the metal ion, Fe^{3+} , leading to the emission quenching. Consequently, this probe **7b** can have potential use as a fluorescent turn-off chemosensor versus Fe^{3+} and Fe^{2+} in different biological and environmental applications.

A photograph of PL emissions of probe **7b** in the presence of various metal ions under the 365 nm UV light was also depicted in Fig. 4. One can see from Fig. 4 that the bluish-green fluorescence intensity of probe **7b** did not show any specific change for most of the metal ions. However, the emission intensity of probe **7b** diminished significantly for Fe^{3+} and less for Fe^{2+} . These results indicate that probe **7b** has a high selectivity towards Fe^{3+} (more strongly) and Fe^{2+} (less). These observations are compatible with the PL measurements in Fig. 3. Therefore, these findings suggest that probe **7b** can find a potential use in chemosensor applications.

The selectivity of probe **7b** towards Fe^{3+} was also investigated in the presence of the other interfering metal cations. As it was depicted in Fig. 5, the PL emission of probe **7b** with the addition of various metal cations did not change (red bars), except for the addition of Fe^{3+} and Fe^{2+} ions (blue bars). In the case of interference studies, when Fe^{3+} ion was separately added into each solution of probe **7b** containing other interfering metal ions, the emission intensity of probe **7b** at 498 nm was significantly quenched (blue bars). These findings imply that probe **7b** is potentially usable for detecting iron ions in aqueous media without being affected by other interfering metal ions.

Sensitivity of Probe **7b**

The sensitivity properties of probe **7b** towards Fe^{3+} and Fe^{2+} were investigated by the fluorescence intensity changes of probe **7b** at 498 nm. For these purposes, increasing concentrations of Fe^{3+} and Fe^{2+} added to probe **7b** (Fig. 6). It was found that the PL emission of probe **7b** at 498 nm decreased for both when the increasing concentrations of Fe^{3+} and Fe^{2+}

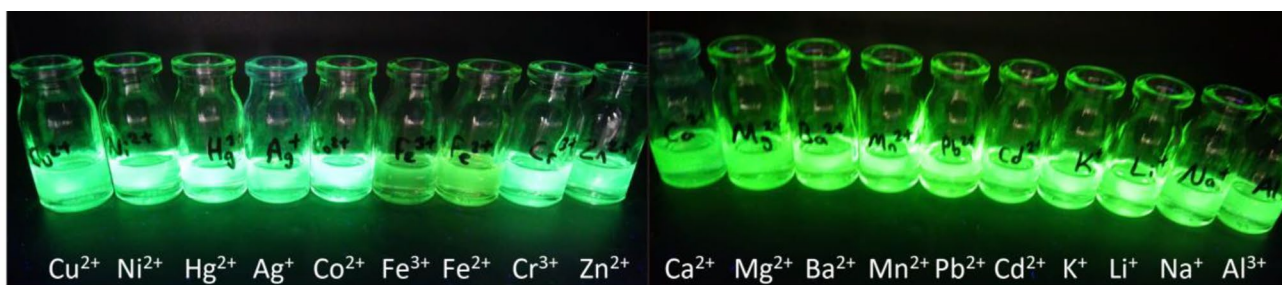


Fig. 4 Photograph of a solution of probe **7b** in the presence of various metal ions under the 365 nm UV light

Fig. 5 The selectivity of probe **7b** in DMSO towards Fe^{3+} in the presence of various interfering metal ions (400 eq.). Black bars show the fluorescent emission of probe **7b**. Red bars show the fluorescent emission of probe **7b** in the presence of different competing metal cations, separately. Blue bars show the fluorescent emission of probe **7b** in the presence of different competing metal cations after the addition of Fe^{3+}

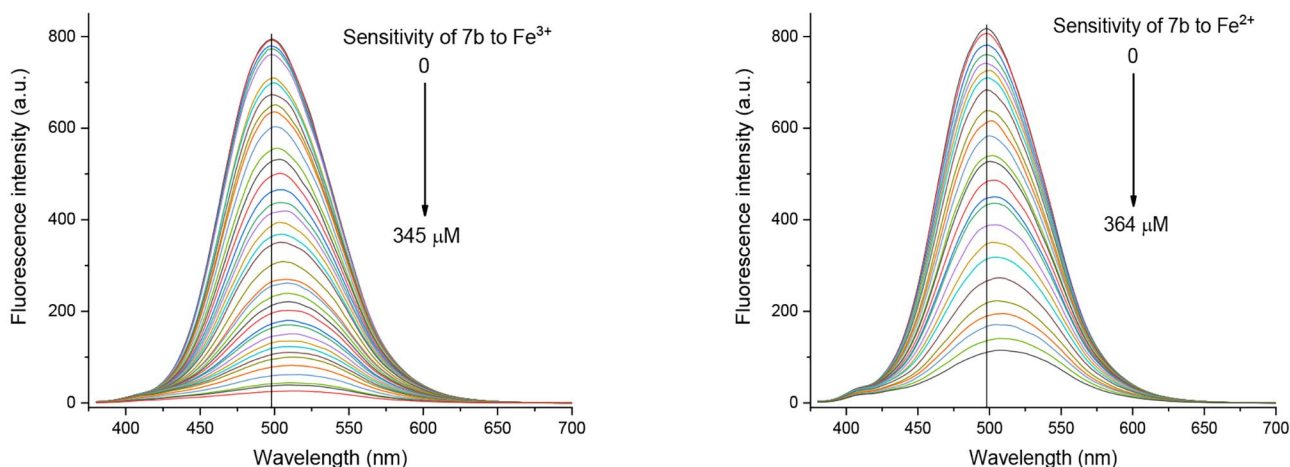
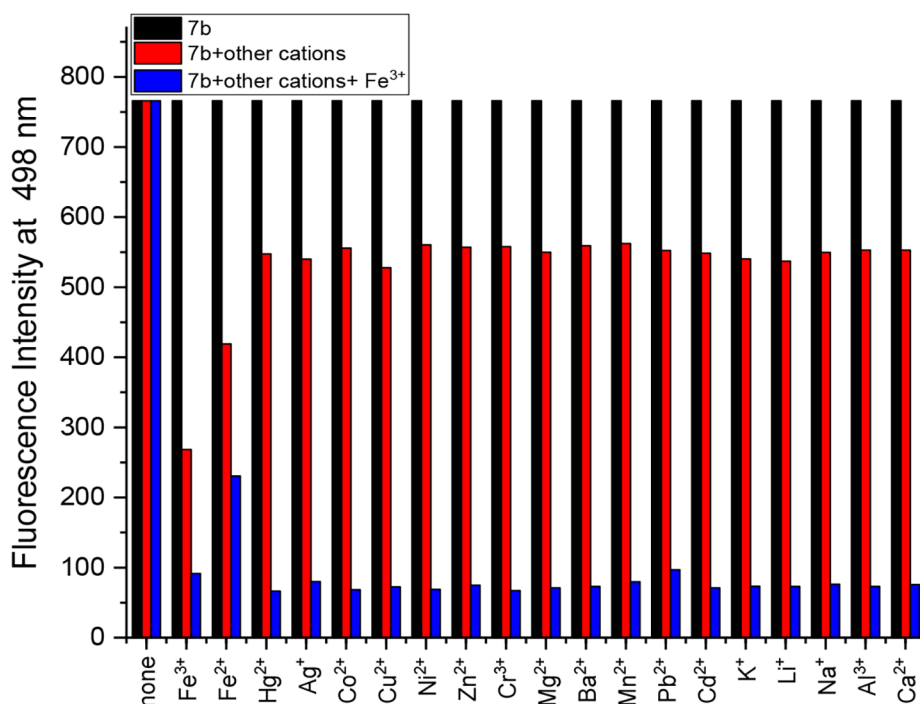


Fig. 6 The fluorescence intensity variation of probe **7b** versus the different concentrations of the added Fe^{3+} (left) and Fe^{2+} (right)

were added. Moreover, no shift in emission maximum at 498 nm occurred even if much more iron ions were added.

Limit of Detection of Probe **7b**

The limit of detection (LOD) was determined as described in previous literature [8–10]. To do this, first fluorescence intensity changes of probe **7b** were plotted against the addition of different iron ion concentrations, as depicted in Fig. 7; then the best linear ranges were selected from this plot. Iron concentrations between 0.008 and $-0.026 \mu\text{M}$ for

Fe^{3+} and $0.166 \mu\text{M} - 1.96 \mu\text{M}$ for Fe^{2+} represent the best linear range. These ranges were plotted as an inset in Fig. 7.

To calculate LOD, the F_0/F ratios were plotted against the concentration ranges of iron ions (Fig. 8), determined from the best linear range of the graph in Fig. 7. This graph is also known as the Stern-Volmer graph, where F_0 represents the emission intensity of probe **7b** and F represents the emission intensity of probe **7b** with the added concentrations of iron ions for the above range. The LOD was then calculated from $3\sigma/S$ Eqs. [8–10, 18, 24, 25], where σ is the standard deviation of the y-intercept and S is the slope of the curve. From

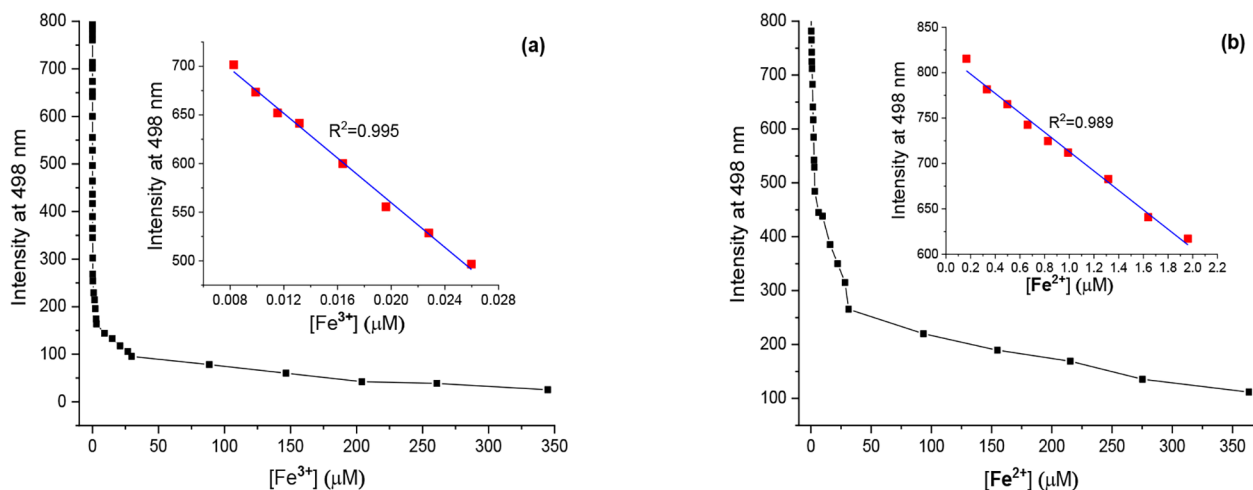


Fig. 7 The maximum fluorescence intensity values of probe **7b** versus different added Fe^{3+} (a) and Fe^{2+} (b) concentrations (inset: the best linear range found in the plot)

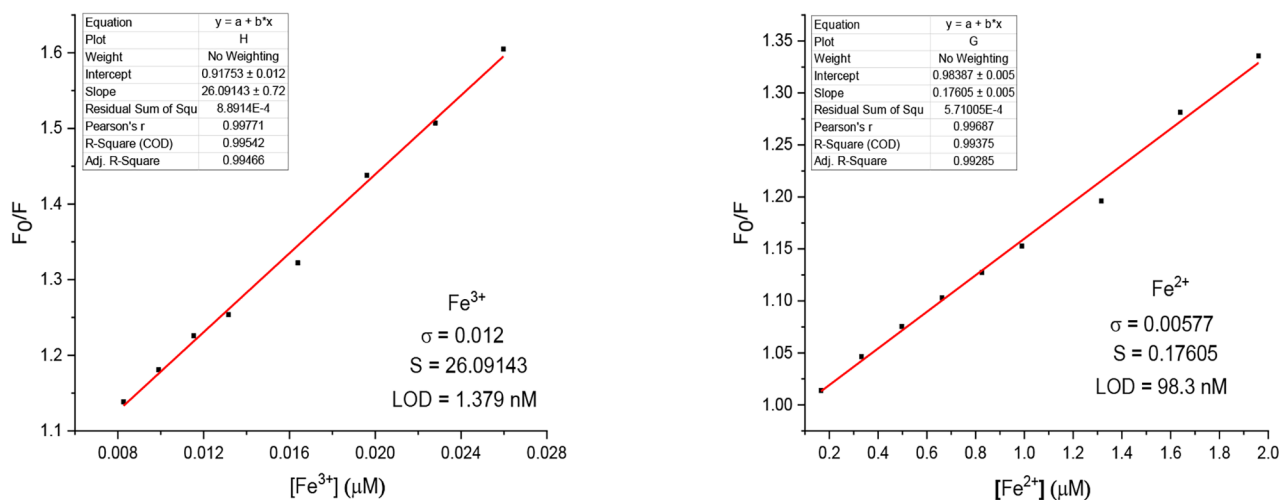


Fig. 8 Stern-Volmer plot for probe **7b** against Fe^{3+} (left) and Fe^{2+} (right)

this, the LOD values were found as $0.00138 \mu\text{M}$ (1.38 nM) for Fe^{3+} and $0.0983 \mu\text{M}$ (98.3 nM) for Fe^{2+} .

According to our best knowledge, this LOD value in detecting Fe^{3+} ion with probe **7b** is the smallest reported so far [6, 13, 26]. This finding looks an exciting observation since the American Environmental Protection Agency (EPA) suggests that the permissible limit level for iron ions in drinking water can be a maximum of $\sim 5.357 \mu\text{M}$ [10, 27]. The LOD value of this study is much smaller than the value of EPA that accepts for drinking water.

Binding Process

Fluorescence intensity measurement studies indicated that the fluorescence intensity of probe **7b** was quenched only by the addition of iron ions. As Fe^{3+} is a paramagnetic

ion, the emission of probe **7b** was probably quenched with paramagnetic effect through electron and/or energy transfer process [6, 7]. The strong paramagnetic effect of Fe^{3+} ion causing quenching of the fluorescence emissions was also observed by others [1, 6, 7, 28, 29]. To determine the binding ratio of the probe **7b** and Fe^{3+} ion, emission intensity of probe **7b** at 498 nm was monitored for continuous variation of molar fraction of Fe^{3+} ion. This is known as Job's plot [30]. For this 1.0×10^{-6} equimolar concentrations of probe **7b** in DMSO and Fe^{3+} in deionised water were prepared and mixed in different volumes (v-v, μL) as follows; 1000–0, 900–100, 800–200, 700–300, 600–400, 500–500, 400–600, 300–700, 200–800, 100–900, 0–1000. A volume of mixture was fixed to 1000 μL , which was further diluted with 2000 μL DMSO. Each mixture corresponds to the following mole fractions of Fe^{3+} ion, respectively:

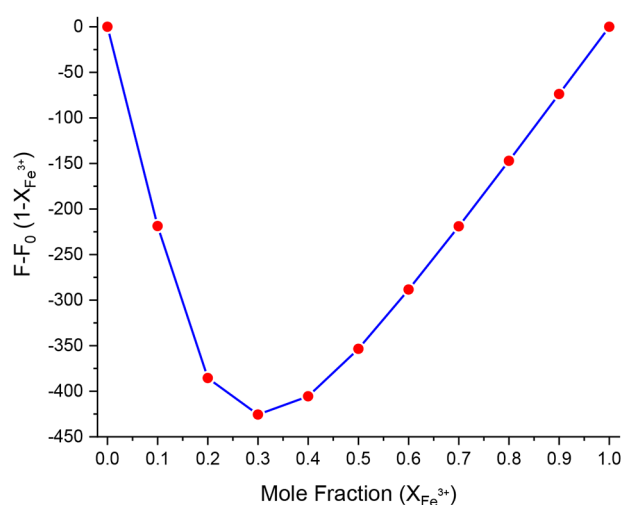


Fig. 9 Job's plot of fluorescence of probe **7b**- Fe^{3+} complex (λ_{exc} :370 nm)

0.0, 0.1, 0.2, 0.3, 0.4, 0.5, 0.6, 0.7, 0.8, 0.9, 1.0. Emission intensity changes ($F - F_0$) at 498 nm, after correction with $(1 - X_{Fe^{3+}})$ [30], were plotted against mole fraction of Fe^{3+} ion, as shown in Fig. 9.

The minimum emission was observed at 0.3 mol fraction of Fe^{3+} and this corresponds to a 2:1 probe **7b**- Fe^{3+} binding ratio (Scheme 2). Probably Fe^{3+} ion complexed to probe **7b** by the oxygen atoms of the aldehyde groups and the nitrogen atoms of the pyridine rings.

To understand the interaction region of probe **7b** with Fe^{3+} ions, FT-IR spectra studies were carried out by using ATR technique (Fig. 10). One can see that C=N stretching

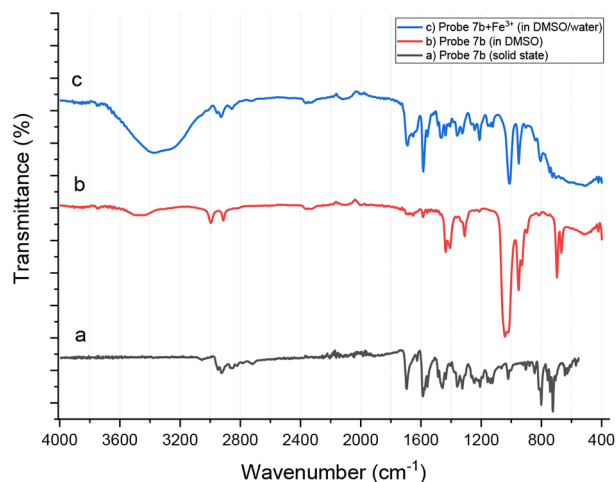
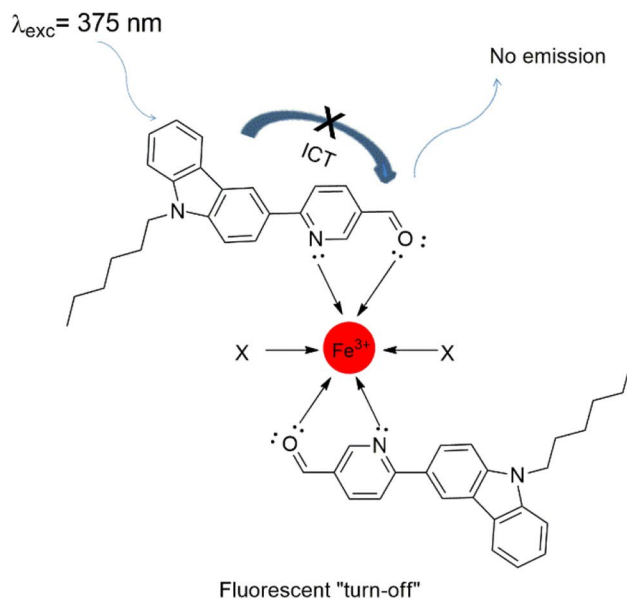
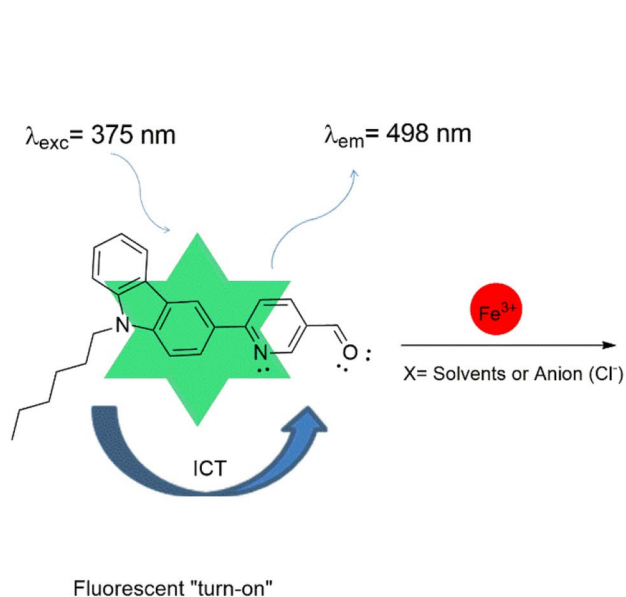


Fig. 10 FT-IR spectra of probe **7b** in a solid state (a), probe **7b** in DMSO (b) and probe **7b**- Fe^{3+} complex in DMSO/water (c)

vibration in the pyridine ring occurs at 1400 cm^{-1} . Upon the addition of Fe^{3+} ions, the peak was shifted from 1400 cm^{-1} to 1600 cm^{-1} . Upon coordination with Fe^{3+} , C=O stretching vibration region would have shifted from 1700 cm^{-1} to higher frequencies ($1750\text{--}1800\text{ cm}^{-1}$). However, in the spectrum no remarkable variation was observed at this region. This result suggests that the more probable coordination of Fe^{3+} is therefore with the nitrogen atom of the C=N moiety of the pyridine ring. Fe^{3+} is a strong Lewis acid; therefore, preferentially it tends to accept the lone pair electrons from the nitrogen atom of the pyridine ring. The broad peak between 3000 and 3800 cm^{-1} is related to



Scheme 2 Plausible probe **7b**-Metal (2:1) interaction

Table 1 Determination of Fe³⁺ ions in real-world water samples

Real samples	Fe ³⁺ added (μM)	Fe ³⁺ found (μM)	Recovery (%)	RSD (%)
7b + Tap water 1	40.00	40.82	102.05	1.35
7b + Tap water 2	60.00	60.88	101.47	0.67
7b + Tap water 3	80.00	79.89	99.87	0.75
7b + Van Lake water 1	50.00	51.41	102.82	2.04
7b + Van Lake water 2	70.00	71.48	102.11	0.87
7b + Van Lake water 3	100.00	100.55	100.55	0.74
7b + Murat River water 1	40.00	40.82	102.05	0.56
7b + Murat River water 2	60.00	59.72	99.53	0.83
7b + Murat River water 3	90.00	91.32	101.47	1.11

O-H stretching vibration of the solvent water. Moreover, the peak observed at 1000 cm⁻¹ is attributed to S=O stretching vibration of the solvent DMSO.

Testing of Real Samples

To check the sensing properties of probe **7b** towards Fe³⁺ in real-world water samples, several fluorescence intensity measurements were carried out by using the spike and recovery method [4, 31–33]. The real-world water samples were taken from three different places in Türkiye. Firstly, 30 μL was taken from each real-world water sample and then added to the solution of probe **7b** in DMSO (1 × 10⁻⁶ M), spiked with various concentrations of Fe³⁺ ions. Finally, the fluorescence measurements of the mixture were recorded. This procedure was repeated for each water sample under the same conditions. All test results were presented in Table 1. The calculated recovery values of these measurements change from 99.87 to 102.82%, depending on the water samples used. The maximum relative standard deviation (RSD) was calculated as 2.04, which is well below the accepted value of 10%. These promising results show that probe **7b** can correctly sense Fe³⁺ ions in real-world water samples. Hence, probe **7b** would be crucial for detecting Fe³⁺ in real-world water samples.

Conclusion

In the present work, previously synthesized 2-(N-hexyl-carbazol-3'-yl)-pyridine-5-carbaldehyde (**7b**) was tested as a novel fluorescent “turn-off” chemosensor. The sensing properties of probe **7b** towards various metal cation ions (Li⁺, Ag⁺, Ba²⁺, Fe³⁺, Cr³⁺ etc.) were investigated. The results showed that probe **7b** has an excellent selectivity and sensitivity towards Fe³⁺ ions over the other interfering metal ions. The emission intensity of probe **7b** decreased significantly by the increasing concentration of Fe³⁺ due to the paramagnetic effect of iron(III) ions. Moreover, it was demonstrated that probe **7b** works very well as a fluorescent

“turn-off” chemosensor under real-world water samples. The LOD value (1.38 nM) is the smallest reported so far for detecting Fe³⁺ ions. Consequently, probe **7b** would be a potential candidate for fluorometric detection of Fe³⁺ in liquid media.

Acknowledgements The authors are grateful to Uludağ University and Atatürk University for the support of this work.

Author Contribution Investigation, Validation, Visualization: [Ahmet Battal], Investigation, Validation, Visualization: [Solomon Bezabeh Kassab], Investigation, Validation, Visualization: [Nuray Altinolcek Gultekin], Conceptualization, Writing - original draft, Supervision: [Mustafa Tavasli], Conceptualization, Writing - original draft, Supervision: [Yavuz Onganer].

Funding This work was supported by Scientific Research Programme (BAP) from Uludağ University [Project #: KUAP (F)-2018/14] and Atatürk University [Project #: FBA-2021-8808].

Data Availability All data generated or analyzed during this study are included in this published article.

Declarations

Conflicts of Interest/Competing Interests The authors declare that they have no conflict of interest.

Ethics Approval Not applicable.

Consent to Participate Not applicable.

Consent for Publication Not applicable.

References

- Kandemir H, Kocak A, Tumay SO, Cosut B, Zorlu Y, Sengul IF (2018) Experimental and theoretical studies of carbazole-based Schiff base as a fluorescent Fe³⁺ + probe. *Turk J Chem* 42
- Yang L, Zhu W, Fang M, Zhang Q, Li C (2013) A new carbazole-based Schiff-base as fluorescent chemosensor for selective detection of Fe³⁺ + and Cu²⁺. *Spectrochim Acta A Mol Biomol Spectrosc* 109:186–192
- Chen J-F, Cheng X-B, Li H, Lin Q, Yao H, Zhang Y-M, Wei T-B (2017) A copillar[5]arene-based fluorescence “on-off-on” sensor is applied in sequential recognition of an iron cation and a fluoride anion. *New J Chem* 41:2148–2153
- Tümay SO, Sarıkaya SY, Yeşilot S (2018) Novel iron(III) selective fluorescent probe based on synergistic effect of pyrene-triazole units on a cyclotriphosphazene scaffold and its utility in real samples. *J Luminescence* 196:126–135
- Pepper SE, Borkowski M, Richmann MK, Reed DT (2010) Determination of ferrous and ferric iron in aqueous biological solutions. *Anal Chim Acta* 663:172–177
- Pundi A, Chang C-J, Chen J, Hsieh S-R, Lee M-C (2021) A chiral carbazole based sensor for sequential “on-off-on” fluorescence detection of Fe³⁺ + and tryptophan/histidine. *Sensors and Actuators B: Chemical* 328
- He W, Liu Z (2016) A fluorescent sensor for Cu²⁺ + and Fe³⁺ + based on multiple mechanisms. *RSC Adv* 6:59073–59080

8. Bayraktutan T, Gur B, Onganer Y (2022) A new FRET-based functional chemosensor for fluorometric detection of Fe³⁺ and its validation through *in silico* studies. *Journal of Molecular Structure*.1256
9. Şenol AM, Onganer Y (2022) A novel “turn-off” fluorescent sensor based on cranberry derived carbon dots to detect iron (III) and hypochlorite ions. *Journal of Photochemistry and Photobiology A: Chemistry*.424
10. Bozkurt E, Arık M, Onganer Y (2015) A novel system for Fe³⁺ ion detection based on fluorescence resonance energy transfer. *Sens Actuators B: Chem* 221:136–147
11. Danjou P-E, Lyskawa J, Delattre F, Becuwe M, Woisel P, Ruelan S, Fourmentin S, Cazier-Dennin F (2012) New fluorescent and electropolymerizable N-azacrown carbazole as a selective probe for iron (III) in aqueous media. *Sens Actuators B: Chem* 171–172:1022–1028
12. Aslandaş AM, Balcı N, Arık M, Şakiroğlu H, Onganer Y, Meral K (2015) Liquid nitrogen-assisted synthesis of fluorescent carbon dots from Blueberry and their performance in Fe³⁺ detection. *Appl Surf Sci* 356:747–752
13. Zhu W, Yang L, Fang M, Wu Z, Zhang Q, Yin F, Huang Q, Li C (2015) New carbazole-based Schiff base: colorimetric chemosensor for Fe³⁺ and fluorescent turn-on chemosensor for Fe³⁺ and Cr³⁺. *J Luminescence* 158:38–43
14. Şenol AM, Onganer Y, Meral K (2017) An unusual “off-on” fluorescence sensor for iron(III) detection based on fluorescein-reduced graphene oxide functionalized with polyethyleneimine. *Sens Actuators B: Chem* 239:343–351
15. Nelson M, Muniyasamy H, Kubendran AM, Balasubramaniam A, Sepperumal M, Ayyanar S (2021) Carbazole based fluorescent chemosensor for the meticulous detection of tryptamine in aqueous medium and its efficacy in cell-imaging and molecular logic gate. *J Mol Liq* 337:116445
16. Tang L, Wu D, Wen X, Dai X, Zhong K (2014) A novel carbazole-based ratiometric fluorescent sensor for Zn²⁺ recognition through excimer formation and application of the resultant complex for colorimetric recognition of oxalate through IDAs. *Tetrahedron* 70:9118–9124
17. Christopher Leslee DB, Karuppanan S, Vengaian KM, Gandhi S, Subramanian S (2017) Carbazole-azine based fluorescence ‘off-on’ sensor for selective detection of Cu²⁺ and its live cell imaging. *Luminescence* 32:1354–1360
18. Chao J, Duan Y, Zhang Y, Huo F, Yin C, Xu M, Li M (2020) A carbazole-based fluorescent probe for ultra-fast detection of ClO⁻ and its application to live cell imaging. *Chem Papers* 74:1171–1176
19. Ho C-L, Wong W-Y, Gao Z-Q, Chen C-H, Cheah K-W, Yao B, Xie Z-Y, Wang Q, Ma D-G, Wang L-X, Yu X-M, Kwok H-S, Lin Z-Y (2008) Red-Light-Emitting Iridium Complexes with hole-transporting 9-Arylcarbazole moieties for Electrophosphorescence Efficiency/Color Purity Trade-off optimization. *Adv Funct Mater* 18:319–331
20. Xu B, Sheibani E, Liu P, Zhang J, Tian H, Vlachopoulos N, Boschloo G, Kloo L, Hagfeldt A, Sun L (2014) Carbazole-based hole-transport materials for efficient solid-state dye-sensitized solar cells and Perovskite Solar cells. *Adv Mater* 26:6629–6634
21. Nepomnyashchii AB, Parkinson BA (2014) Contrasting electrogenerated chemiluminescence for a dissolved and surface-attached carbazole thiophene cyanoacrylate dye. *ACS Appl Mater Interfaces* 6:14881–14885
22. Altinolcek N, Battal A, Tavasli M, Peveler WJ, Yu HA, Skabara PJ (2020) Synthesis of novel multifunctional carbazole-based molecules and their thermal, electrochemical and optical properties. *Beilstein J Org Chem* 16:1066–1074
23. Misra R, Mandal A, Mukhopadhyay M, Maity DK, Bhattacharyya SP (2009) Spectral signatures of intramolecular charge transfer process in β-Enaminones: a combined experimental and theoretical analysis. *J Phys Chem B* 113:10779–10791
24. Liu L, Liu X, Guo C, Fang M, Li C, Zhu W (2021) Carbazole-based dual-functional chemosensor: colorimetric sensor for Co²⁺ and fluorescent sensor for Cu²⁺ and its application. *J Chin Chem Soc* 68:2368–2377
25. Zhao H-W, Wu G, Sun X-Y, Chao J-B, Li Y, Jiang L, Han H (2018) A highly selective and ratiometric molecular probe for cyanide sensing based on a phenothiazine-hemicyanine dye. *J Luminescence* 201:474–478
26. Karuk Elmas SN, Gunay IB, Genc HN, Aydin D, Arslan FN, Sadi G, Sirit A, Yilmaz I (2020) A tetraoxacalix[2]arene[2]triazine based fluorogenic probe for the sensing of Fe³⁺: computational and living-cell imaging applications. *Journal of Photochemistry and Photobiology A: Chemistry*.403
27. Zhang Y, Wang G, Zhang J (2014) Study on a highly selective fluorescent chemosensor for Fe³⁺ based on 1,3,4-oxadiazole and phosphonic acid. *Sens Actuators B: Chem* 200:259–268
28. Bao X, Cao X, Nie X, Xu Y, Guo W, Zhou B, Zhang L, Liao H, Pang T (2015) A new selective fluorescent chemical sensor for Fe³⁺ based on rhodamine B and a 1,4,7,10-tetraoxa-13-azacyclopentadecane conjugate and its imaging in living cells. *Sens Actuators B: Chem* 208:54–66
29. Zhang Z, Li F, He C, Ma H, Feng Y, Zhang Y, Zhang M (2018) Novel Fe³⁺ + fluorescence probe based on the charge-transfer (CT) molecules. *Sens Actuators B: Chem* 255:1878–1883
30. Şenkuytu E, Eçik ET, Çoşut B (2018) Bodipy decorated triazine chemosensors for Ag⁺ ions with high selectivity and sensitivity. *J Luminescence* 203:639–645
31. Immanuel David C, Prabakaran G, Karuppasamy A, Veetil JC, Kumar RS, Almansour AI, Perumal K, Ramalingan C, Nandhakumar R (2022) A single carbazole based chemosensor for multiple targets: sensing of Fe³⁺ and arginine by fluorimetry and its applications. *J Photochem Photobiol A* 425:113693
32. Yang M, Sun M, Zhang Z, Wang S (2013) A novel dansyl-based fluorescent probe for highly selective detection of ferric ions. *Talanta* 105:34–39
33. Patil SK, Das D (2020) A novel rhodamine-based optical probe for mercury(II) ion in aqueous medium: a nanomolar detection, wide pH range and real water sample application. *Spectrochim Acta Part A Mol Biomol Spectrosc* 225:117504

Publisher’s Note Springer Nature remains neutral with regard to jurisdictional claims in published maps and institutional affiliations.

Springer Nature or its licensor (e.g. a society or other partner) holds exclusive rights to this article under a publishing agreement with the author(s) or other rightsholder(s); author self-archiving of the accepted manuscript version of this article is solely governed by the terms of such publishing agreement and applicable law.